# Investigation of green properties of iron/jet-milled grey cast iron compacts by response surface method

Abdollahi, H., Mahdavinejad, R., Ghambari, M. & Moradi, M.

**Author post-print (accepted) deposited by Coventry University's Repository**

**Original citation & hyperlink:**
Abdollahi, H, Mahdavinejad, R, Ghambari, M & Moradi, M 2014, 'Investigation of green properties of iron/jet-milled grey cast iron compacts by response surface method', Proceedings of the Institution of Mechanical Engineers, Part B: Journal of Engineering Manufacture, vol. 228, no. 4, pp. 493-503.
https://dx.doi.org/10.1177/0954405413502023

DOI 10.1177/0954405413502023
ISSN 0954-4054
ESSN 2041-2975

Publisher: SAGE Publications

**Copyright © and Moral Rights are retained by the author(s) and/ or other copyright owners. A copy can be downloaded for personal non-commercial research or study, without prior permission or charge. This item cannot be reproduced or quoted extensively from without first obtaining permission in writing from the copyright holder(s). The content must not be changed in any way or sold commercially in any format or medium without the formal permission of the copyright holders.**

**This document is the author's post-print version, incorporating any revisions agreed during the peer-review process. Some differences between the published version and this version may remain and you are advised to consult the published version if you wish to cite from it.**

# Investigation of green properties of iron/jet milled grey cast iron compacts by response surface method

Hadi Abdollahi[1*], Ramezanali Mahdavinejad[2], Mohammad Ghambari[3], Mahmoud Moradi[4]

[1*] School of Mechanical Eng., University of Tehran, Iran. habdollahi@ut.ac.ir.

[2] School of Mechanical Eng., University of Tehran, Iran.

[3] School of Metallurgy and Materials Eng., University of Tehran, Iran.

[4] School of Mechanical Eng., University of Malayer, Iran.

## Abstract

Grey cast iron powder was produced from grey cast iron scraps by jet milling method and mixed with commercial pure iron powder. The morphology of the produced powders and characteristics of the powder mixtures were investigated. The mathematical models were successfully developed to predict green properties of iron/jet milled grey cast iron compacts using response surface methodology (RSM). Using RSM the effects of the percentage of jet milled cast iron powder and compaction pressure on green density, green strength and hardness of the green compacts were analyzed and the optimal combinations of the input process parameters were obtained to maximize the responses. The main and interaction effects of the input process parameters and also the validity of the models were evaluated by using analysis of variance (ANOVA) method. Scanning electron microscopy (SEM) micrographs of the powders and the fracture surfaces were provided to discuss the obtained responses. The results indicated that, in addition to fast production rate and economical considerations, the iron/jet milled grey cast iron powder compacts have adequate green properties for the most of different combinations of the input process parameters.

**Keywords**
Grey cast iron, jet milling, response surface methodology (RSM), green properties, ANOVA

## 1. Introduction

The first step to produce parts using powder metallurgy is powder production. It is well known that machining processes are performed on 50-80% of the semi-finished components and in each machining process up to 80% of their materials is transformed into swarfs [1]. Hence, from an economical point of view, it is an interesting idea to comminute these swarfs into useable powders for powder metallurgy process. Among the ferrous scraps, cast iron scrap has a high

potential for this application due to huge quantity of generation, low cost, brittle nature, small chip size and no lubricants impurity. Mechanical comminution of scraps is one of the methods for recycling cast iron scraps to suitable powders to be processed by powder metallurgy method [2]. Different techniques can be used for mechanical comminution of the scraps such as ball milling, hammer milling, vibratory mills, etc. [3-6].

Although the mentioned methods have been reported as successful methods for producing the powders, on an industrial scale, the productivity of these methods is clearly too low. These methods are very time consuming and there is a need for secondary operations such as annealing on the powders [4]. Recently, a new method called “target jet milling” has been developed by Ghambari et al. [7] in which grey cast iron scraps are transformed into useable powders for powder metallurgy processing with a very high rate. The produced powders do not need secondary operations such as annealing, etc. In their work, cast iron scraps are accelerated by a high speed air jet, clashed to a target plate and fragmented. They obtained the optimal parameters for jet milling process of grey cast iron scraps. In another work, Emadi et al. [8] investigated physical properties of the powders produced by jet milling and ball milling methods and studied mechanical properties of PM parts produced from the powders. They concluded that the powders produced by jet milling method have sharper edges than the powders produced by ball milling method along with more compressibility.

Mixing a cast iron powder with an iron powder makes it possible to produce an alloyed powder metallurgy part of high wear resistance and good physicomechanical properties. Simultaneously, this is accompanied with economical iron powder consumption that is more expensive than grey cast iron. The addition of a grey cast iron powder obtained by traditional milling methods to an iron powder is reported in various references [9-12].

Mathematical and statistical techniques are widely used for optimization and prediction of production process parameters. These techniques include design of experiments (DOE), regression analysis and analysis of variance (ANOVA). Response surface methodology (RSM) is one of the DOE approaches which offers various desirable characteristics such as proper reduction in the number of experiments, consideration of the interaction effects and development of the mathematical functions to achieve a logical relationship between the input and output parameters. RSM is widely used for optimization of the production processes such as machining, forging, welding, casting, injection molding, etc [13-17]. Meanwhile, powder metallurgy process is not an exception to this rule and some research are conducted on this process using mathematical and statistical approaches [18-21].

In the traditional methods very time consuming and expensive milling methods are used for producing the grey cast iron powder from the scraps. Moreover, in many cases the green properties of the produced compacts are not suitable for industrial applications. In this study, grey cast iron scraps are transformed into powder by jet milling as a very fast milling method and then mixed with iron powder in different ratios and compacted under different compaction pressures. Green properties of these compacts are investigated and optimized by RSM in order to evaluate their potential for cost effective usages in industrial scales. SEM micrographs are presented to discuss the validity of the obtained results.

## 2. Experimental procedure and design

The first row material used in this study was pearlitic lamellar grey cast iron scrap which was obtained from dry turning of car engine components. The chemical composition of grey cast iron scrap is reported in Table 1. The morphology and size of the scraps are shown in SEM

micrographs of Figures 1(a) and (b). Target jet milling method was used for pulverizing the scraps. The optimized parameters of the previous work on target jet milling were applied to achieve the best results for pulverizing the scraps [7]. Accordingly, in order to obtain enough grey cast iron powder with appropriate size distribution, the amount of 5 kg of initial scraps was subjected to five cycles of jet milling at a feed rate of 40 gr/s, impact angle of 90°, the nozzle to target distance of 8 cm and under compressed air with the pressure of 0.6 MPa. After five jet milling cycles, particle size distribution of the powders was obtained as given in Table 2. The powders with size less than 180µm were separated by sieving because of wide industrial applications of this particle size range distribution [22]. Table 2, also reports the final particle size distribution of the used grey cast iron powder for producing the powder metallurgy parts. Particle size distribution and chemical-physical properties of the commercial pure iron powder are given in Tables 1 and 2.

**Table 1.** Chemical composition of the used materials

| Chemical composition of grey cast iron scrap | | | | | | | | |
|---|---|---|---|---|---|---|---|---|
| Element | C | Si | Mn | Cr | S | Sn | P | Cu |
| wt.% | 3.3-3.5 | 2.0-2.2 | 0.55-0.75 | 0.06-0.12 | 0.06-0.09 | 0.01-0.03 | <0.05 | <0.02 |
| Chemical composition of commercial iron powder | | | | | | | | |
| Element | C | Si | P | S | Mn | Fe | | |
| wt.% | 0.02 | 0.05 | 0.015 | 0.015 | 0.15 | R | | |

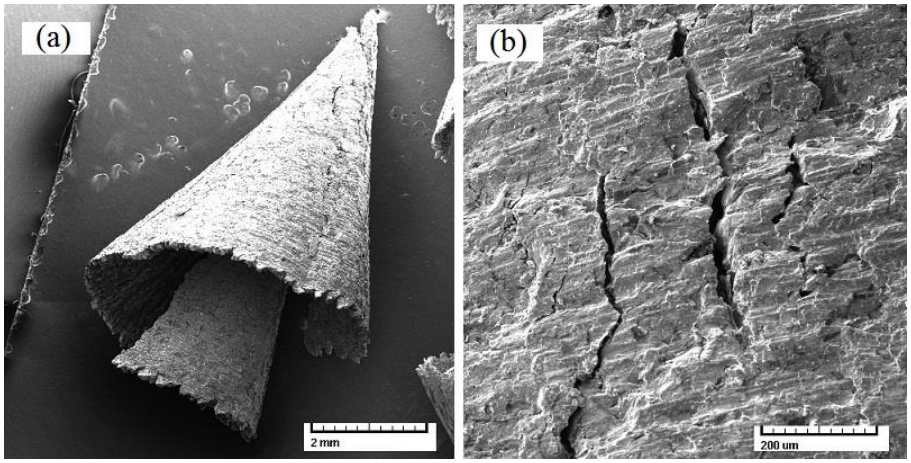


**Figure 1.** SEM micrographs showing: (a) morphology of the grey cast iron scrap, and (b) surface of the same scrap.

**Table 2.** Particle size distribution of the used powders

| Particle size distribution after 5 jet milling cycles of 5 kg grey cast iron scraps | | | | | |
|---|---|---|---|---|---|
| Particle size(µm) | 250-600 | 106-250 | 75-106 | 45-75 | -45 |
| Fraction(%) | 63.7 | 26.4 | 5.6 | 2.8 | 1.5 |
| Particle size distribution of used jet milled grey cast iron powder | | | | | |
| Particle size(µm) | 106-180 | 75-106 | 45-75 | -45 | |
| Fraction(%) | 62.08 | 21.42 | 10.77 | 5.73 | |
| *Apparent Density: 2.56 gr/cm$^3$* | | *Flow Rate(Hall): 39.51 s/50gr* | | | |
| Particle size distribution of commercial iron powder | | | | | |
| Particle size(µm) | 106-180 | 75-106 | 45-75 | -45 | |
| Fraction(%) | 34.17 | 22.43 | 32.26 | 11.14 | |
| *Apparent Density: 3.11 gr/cm$^3$* | | *Flow Rate(Hall): 24.55 s/50gr* | | | |

After preparation of the powders, mixtures of iron powder/jet milled grey cast iron powder were prepared in proportions of 30/70, 40/60, 50/50, 60/40 and 70/30. Flow rate and apparent density of the mixtures were determined using Hall flowmeter according to ASTM B213-97 and ASTM B212-99, respectively. Prepared mixtures were uniaxially compacted under pressures of 400, 500, 600, 700 and 800 MPa inside a die with a rectangular hole with dimensions of 12.7 and 31.7 mm. Die wall lubrication was carried out by 10% zinc stearate solution during the compacting process according to ASTM B331-95. Compressibility of the mixed powders was determined by measuring and weighting the compacted specimens according to ASTM B331-95. Brinell hardness tests were carried out by applying a load of 30 kg to the polished surface of the compacts through a ball of 2.5 mm diameter according to ASTM E10-12. Green strength of the compacts was determined by three points bending test on rectangular specimens using SANTAM-50 testing machine at room temperature according to ASTM B312-96. Scanning electron microscopy in an MV2300 type instrument was used to examine the morphology of the scraps, powders and fracture surface of green compacts.

In the present work, the experiments were designed based on a Central Composite Design (CCD) five-level RSM method [23]. Cast iron powder percentage (30 to 70%) and compaction pressure (400 to 800 MPa) were selected as process independent variables. The process input variables and experimental design levels illustrated with coded and actual values are given in Table 3. The upper and lower levels of the parameters are coded as +2 and −2, respectively, and the coded values of any intermediate levels are calculated using the following expression [23]:

$$X_i = \frac{2X - (X_{\max} + X_{\min})}{(X_{\max} - X_{\min})/2} \tag{1}$$

Where $X_i$ is the required coded value of a factor of any value $X$ from $X_{min}$ to $X_{max}$, where $X_{min}$ and $X_{max}$ are the lower and upper limits of the factors, respectively.

**Table 3.** Independent process parameters and their levels

| Variable | Notation | Unit | Levels | | | | |
|---|---|---|---|---|---|---|---|
| | | | -2 | -1 | 0 | 1 | 2 |
| cast iron powder percentage | CIP | [-] | 30 | 40 | 50 | 60 | 70 |
| compaction pressure | P | [MPa] | 400 | 500 | 600 | 700 | 800 |

The responses measured are green density (to evaluate compressibility), green strength and hardness. The designed matrix and the observed data for different settings of the process parameters are reported in Table 4. Experimental design includes four experiments as factorial points in cubic vertex, four experiments as axial points and five experiments in the cubic centre as centre points experiments.

**Table 4.** Design matrix, expressed by two input process parameters as design levels and the responses

| Experiment No. | Run Order | CIP [-] | P [-] | Green Density[gr/cm$^3$] | Compression Ratio($C_R$) | Green Strength[MPa] | Hardness [BHN] |
|---|---|---|---|---|---|---|---|
| 1 | 13 | 0 | 0 | 5.90 | 2.07 | 5.97 | 39.35 |
| 2 | 1 | -1 | -1 | 5.83 | 2.01 | 4.86 | 35.48 |
| 3 | 4 | -1 | 1 | 6.21 | 2.14 | 8.83 | 43.65 |
| 4 | 2 | 1 | -1 | 5.58 | 2.00 | 3.41 | 29.98 |
| 5 | 12 | -2 | 0 | 6.11 | 2.06 | 7.46 | 37.31 |
| 6 | 6 | 2 | 0 | 5.68 | 2.07 | 4.60 | 32.09 |
| 7 | 3 | 0 | 0 | 5.89 | 2.07 | 5.88 | 39.23 |
| 8 | 10 | 0 | 0 | 5.95 | 2.09 | 5.95 | 39.07 |
| 9 | 5 | 1 | 1 | 6.04 | 2.16 | 7.47 | 43.06 |
| 10 | 9 | 0 | 0 | 5.91 | 2.07 | 5.94 | 39.48 |
| 11 | 11 | 0 | -2 | 5.25 | 1.84 | 2.28 | 27.67 |
| 12 | 8 | 0 | 2 | 6.32 | 2.21 | 12.85 | 49.12 |
| 13 | 7 | 0 | 0 | 5.84 | 2.05 | 5.85 | 39.16 |

## 3. Results and discussion

### 3.1. Powder characterization

Figure 1(a) shows the morphology of a typical machining scrap used in this work. As it can be seen, the scrap is a kind of distinct conical-helical. Also, Figure 1(b) illustrates the same scrap with a higher magnification and indicates the presence of a few fine and largish cracks on the surface of the scrap. Existence of these cracks facilitates the milling and comminution of the scraps in jet milling process. On the other hand, cast iron matrix includes free graphite flakes which act as internal notches and lead to easier fracturing of the scraps [24]. Figure 2(a) shows the SEM micrograph of the produced powders by jet milling method. As demonstrated, these powders are mostly in flake, irregular and angular shapes. The morphology properties of the powders are resultant of the inherent property of the jet milling method that influences particle shape and surface topography [8]. Figure 2(b) represents an individual particle with a higher

magnification. According to Figure 2, the produced powders have roughened surfaces with sharp edges that influence the frictional forces between the particles. Such effects are important in the case of bulk movement of the powders, when the powder is flowing, settling or during compaction. The extent of the actual particle-to-particle contact during sintering is also affected by the nature of the surface roughness [25].

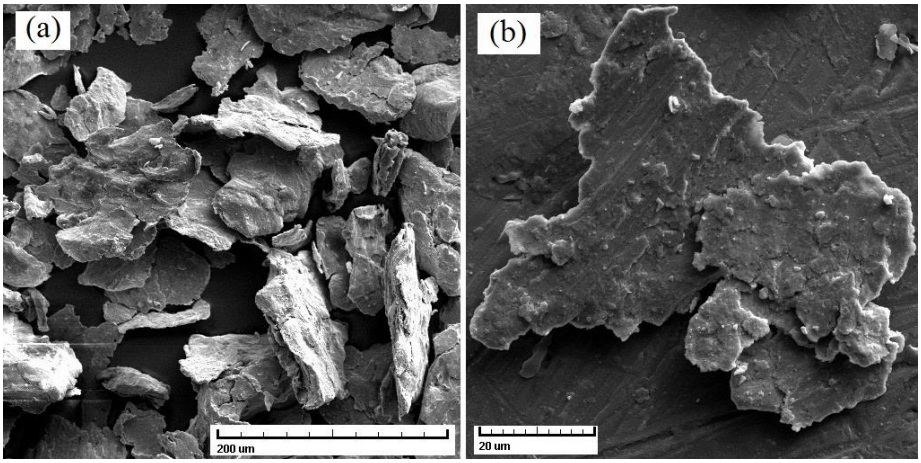


**Figure 2.** SEM micrographs showing: (a) grey cast iron powders produced by jet milling method, and (b) a magnificated particle of the same powders.

Apparent density is a critical characteristic of a powder with the application in tooling design which provides enough fill to produce a part with desired compacted density, while adequate flow of the powder determines the filling speed and is required for a rapid fill [25]. As illustrated in Figure 3, the apparent density and flow time, decreases and increases with the increase of the cast iron powder, respectively. The first reason behind these trends is the irregular and flake shape, sharp edges, large surface area and the roughened surface of the powders which results in the increase of the frictional forces between the particles [25]. The second reason is attributed to iron and cast iron particles size distribution. The particle size distributions are compared in Table 2; it indicates that the cast iron powders are relatively coarser than iron powders; when a coarse

size powder proportion increases, because of the decrease of the apparent density, the flow time increases regardless of the particles shape (i.e. irregular or spherical) [1].

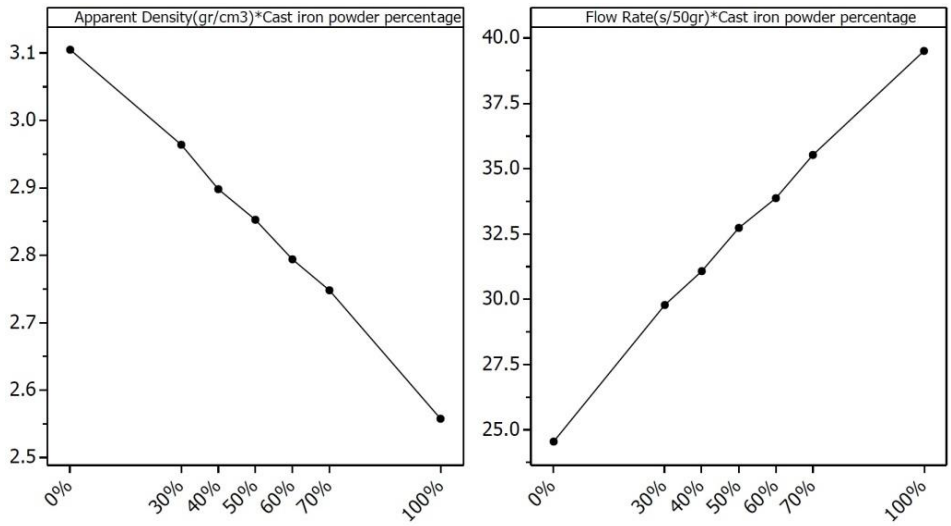


**Figure 3.** Effect of grey cast iron powder percentage on apparent density and flow rate of the powder mixtures.

## 3.2. Compressibility

Compressibility is defined as the ability of a powder to be reduced to a lower volume under compaction pressures. Therefore, compressibility of a powder is an important factor in the design of pressing tools and achieving desirable component density [26]. In this study, green densities (see Table 4) are considered as compressibility criterions and a full quadratic polynomial model is used to analyze the compressibility. The results of ANOVA run on green density after deleting insignificant terms are given in Table 5. According to Table 5, all main parameters are significant and among quadratic terms, the quadratic term $P^2$ has a significant effect. This is determined by sufficient low P-values below 0.05 in ANOVA tables. The other terms are insignificant. Moreover, T-values of the significant parameters indicate that the influence of compaction pressure on the compressibility is about 2.3 times higher than that of the cast iron

powder percentage. The high value of adjusted correlation coefficient ($R^2$(adj.)=96.96%) indicates the excellent fitness for regression model. Meanwhile, the lack-of fit is insignificant. It should be emphasized that in ANOVA, the best situation occurs when the regression model is significant and lack-of fit is insignificant at the same time [23]. All of the above considerations indicate an excellent adequacy of the regression model. Finally, according to the analysis of the results the final regression equation for green density is given as Equation 2, where it is described in terms of the coded values of the parameters.

$$D = 5.912 - 0.107CIP + 0.248P - 0.029P^2 \quad (2)$$

**Table 5.** Modified analysis of variance for green density

| Source of variation | Sum of squares | Degrees of freedom | Mean squares | *T* value | *F* value | *P* value |
|---|---|---|---|---|---|---|
| Regression | 0.896670 | 3 | 0.298890 | - | 128.41 | 0.000 |
| CIP | 0.136320 | 1 | 0.136320 | -7.653 | 58.57 | 0.000 |
| P | 0.739537 | 1 | 0.739537 | 17.825 | 317.73 | 0.000 |
| P×P | 0.020813 | 1 | 0.020813 | -2.990 | 8.94 | 0.015 |
| Residual Error | 0.020948 | 9 | 0.002328 | - | - | - |
| Lack-of-Fit | 0.015099 | 5 | 0.003020 | - | 2.07 | 0.251 |
| Pure Error | 0.005849 | 4 | 0.001462 | - | - | - |
| Total | 0.917618 | 12 | - | - | - | - |
| $R^2$ = 97.72% | $R^2$ (adj) = 96.96% | | | | | |

The normal probability plot for the response green density is shown in Figure 4(a). It is evident that residuals are scattered on the straight line and the errors have a normal distribution on the normal probability plot [27]. Thus, the extracted regression model is adequate for the prediction of the parameters effects.

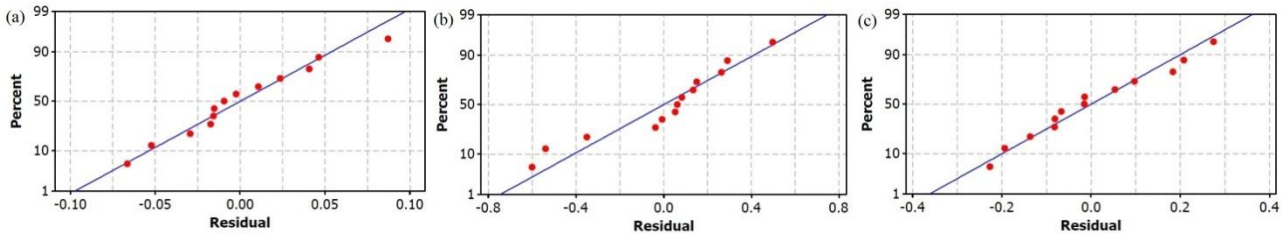


**Figure 4.** Normal probability plots for: (a) green density, (b) green strength, and (c) hardness.

Figure 5 illustrates response surface plot and contour plot for green density. It is clear that, the green density increases by decreasing the cast iron powder percentage and increasing the compaction pressure. Improving density with increased compaction pressure is an obvious rule in powder metallurgy technology [28]. However, the major reason for reduction of green density with increased cast iron powder is related to the particle shape of the cast iron powders mixed with the iron powders. Since the cast iron powders are irregular, flake, angular and surface roughened, the interparticle friction is magnified and the particles do not rearrange themselves easily which leads to lower values of the compressibility. It is noticeable that another key factor influencing the compressibility is the particles size. In the case of coarse powders, due to the reduced number of contact points between the particles the interparticle friction decreases, which in turn, results in the easier rearrangement of the particles and the improved compressibility. In this work, the largish particle size of cast iron powder than iron powder has partly compensated the unfavorable influence of the irregular powders on the compressibility. The other reason for decreasing green density with increased cast iron powder is the addition of the hard powder to the soft powder. In a hard-soft powder mixture, the low amount of the hard powder has not a significant effect on the compressibility, but with the increase of the amount of the hard powder, the hard powders form a continuous skeleton inter compaction die and, therefore, decrease the compressibility strongly[29]. In this case, the coarse hard particles have a less adverse effect on

the compressibility than the fine powders. Therefore, from this point of view, selection of a largish particle size of the cast iron powder than the iron powder has also decreased the adverse effect of the hard powders on the compressibility.

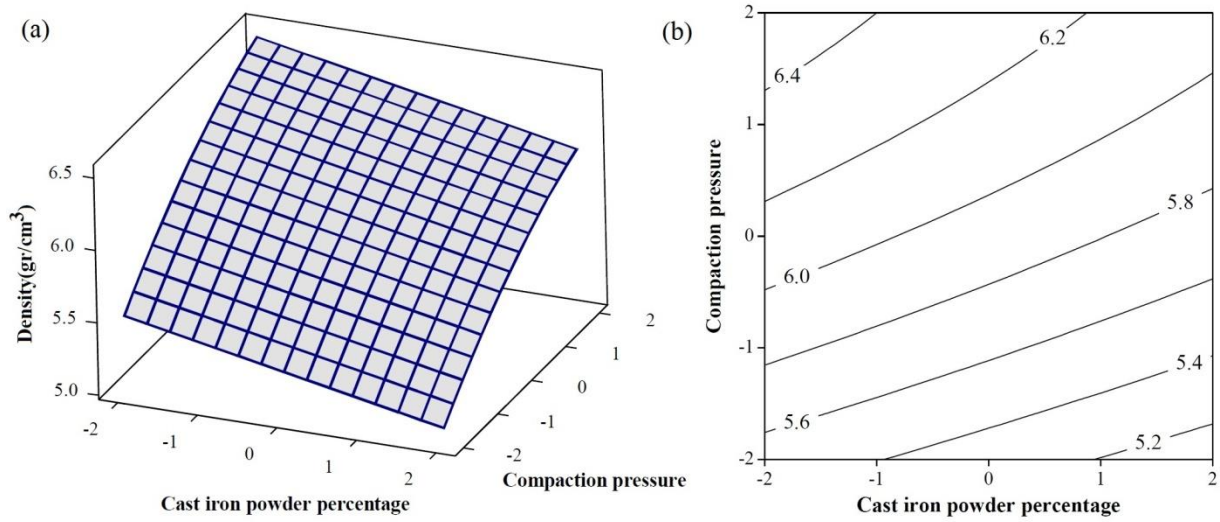


**Figure 5.** (a) Surface plot, and (b) contour plot, for green density.

Another investigated characteristic of the mixtures is compression ratio ($C_R$). The ratio of apparent density of the powder to green density is called compression ratio and is used to find the fill depth. The fill depth to produce a part with required thickness is determined by multiplying the finished part thickness by $C_R$ of the powder to be compacted [25]. Compression ratios for different iron/jet milled grey cast iron powder mixtures are reported in Table 4. A low compression ratio is desirable because of tooling and production rate considerations.

### 3.3. Green strength

Green strength is a very important characteristic of green compacts that determines the ability of a green compact to retain its size and shape for safe handling before sintering [26]. The results of ANOVA run on green strength are given in Table 6. Also, Figure 4(b) illustrates the normal

probability plot for green strength that does not reveal any unusual problem as was discussed in the previous section. Equation 3 shows the final regression equation for green strength.

$$S = 5.88 - 0.71CIP + 2.43P + 0.4P^2 \quad (3)$$

**Table 6.** Modified analysis of variance for green strength

| Source of variation | Sum of squares | Degrees of freedom | Mean squares | T value | F value | P value |
|---|---|---|---|---|---|---|
| Regression | 80.9813 | 3 | 26.9938 | - | 197.62 | 0.000 |
| CIP | 6.0634 | 1 | 6.0634 | -6.663 | 44.39 | 0.000 |
| P | 70.9074 | 1 | 70.9074 | 22.784 | 519.12 | 0.000 |
| P×P | 4.0105 | 1 | 4.0105 | 29.36 | 5.419 | 0.000 |
| Residual | 1.2293 | 9 | 0.1366 | - | - | - |
| Lack-of-Fit | 1.2190 | 5 | 0.2438 | - | 94.87 | 0.000 |
| Pure Error | 0.0103 | 4 | 0.0026 | - | - | - |
| Total | 82.2106 | 12 | - | - | - | - |
| $R^2$ = 98.50% | $R^2$ (adj) = 98.01% | | | | | |

The corresponding dependency of green strength variation on independent variables is illustrated in Figure 6. The green strength increases as the compaction pressure increases and the cast iron powder percentage decreases. The increase of the green strength with increased compaction pressure is expectable. However, decreasing green strength with increased cast iron powder is due to the more hardness of the cast iron powder with respect to that of the iron powder. Considering the green density as the first determinant cause of the green strength, the increase of the cast iron powder decreases the green density and leads to decrease in the green strength; on the other hand, particle characteristics such as irregular shape and rough surface of particles are key factors that improve the green strength through increasing the mechanical interlocking [30]. Since the cast iron powders produced by jet milling method have the mentioned characteristics, in spite of their more hardness and larger sizes than iron powder, they result in the compacts with adequate green strengths. Another reason for achieving adequate green strength in these mixtures

is the fact that due to the specifications of jet milling procedure, the amount of free graphite on the surface of the cast iron powders is low. It is noticeable that existence of additives such as graphite prevents mechanical interlocking. The SEM micrographs of the fracture surfaces of the typical mixtures shown in Figure 7 confirm the results. The compact including 50% cast iron powder pressed at 800 MPa has an almost entirely transgranular failure on the fracture surface which is due to the high compaction pressure. This is the compact that has the highest green strength of 12.85 MPa among all the specimens of Table 4. The low green strength means that plastic deformation of the particles happens without occurring cold weld between them and the interparticle attraction force is weak as depicted in Figures 7 (b) and (c). Furthermore, both intergranular and transgranular failures can be seen in Figure 7 (b), where the former is due to the high amount of cast iron powder and the latter is due to the high compaction pressure. This compact is the one that has the green strength of 7.47 MPa. Also, Figure 7 (c) exhibits a completely intergranular failure with the large pores between the particles for the mixture including 70% cast iron powder pressed at 600 MPa which is the result of high amount of the cast iron powder in the mixture. This compact has the green strength of 4.60 MPa.

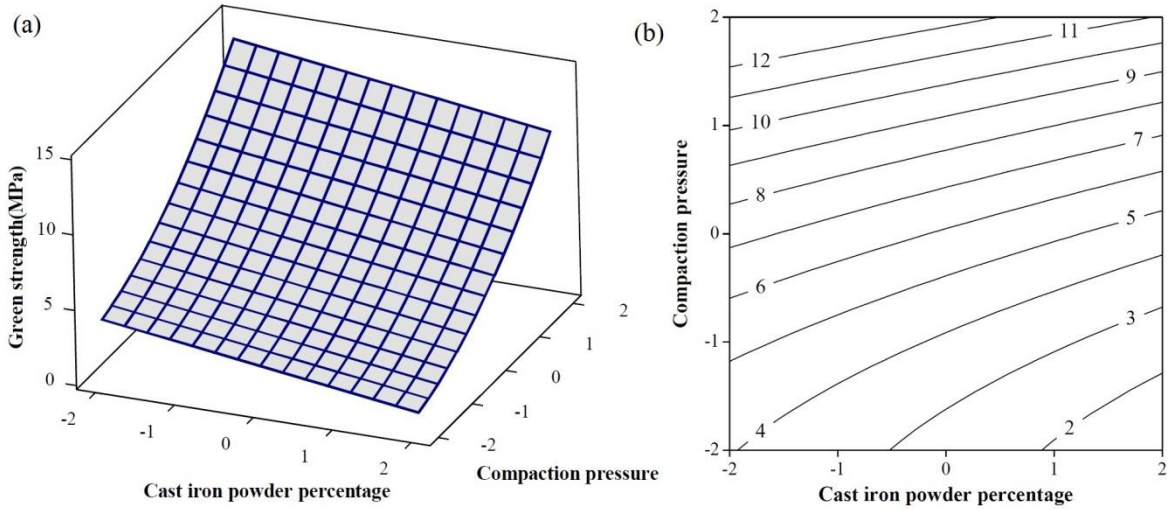


**Figure 6.** (a) Surface plot, and (b) contour plot, for green strength.

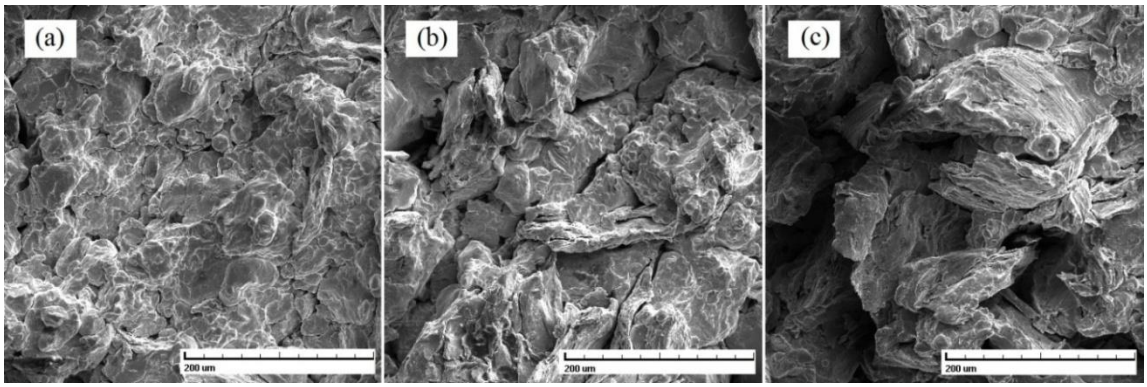


**Figure 7.** SEM fractographs of: (a) the mixture including 50% cast iron powder pressed at 800 MPa (row 12 of Table 4), (b) the mixture including 60% cast iron powder pressed at 700 MPa (row 9 of Table 4), and (c) the mixture including 70% cast iron powder pressed at 600 MPa (row 6 of Table 4).

Now, the important problem is determination of the desired combinations of jet milled grey cast iron powder percentage-compaction pressure in order to obtain an acceptable green strength for handling requirements. According to [22], a minimum green strength of 5.5 MPa is required for secure handling of green compacts before sintering. Figure 8 shows the overlaid contour plot for the green strength versus two variable parameters. The white area illustrates the desirable criteria of the parameters that results in green strengths higher than 5.5 MPa. This result shows the high ability of jet milled grey cast iron scraps for mixing with an iron powder to produce powder metallurgy parts with different combinations of cast iron powder percentage-compaction pressure and different sintered properties along with economical considerations.

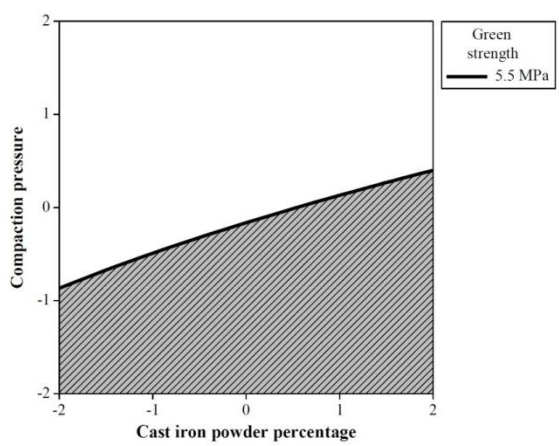


**Figure 8.** Overlaid contour plot for green strength.

3.4. Hardness

The results of ANOVA for the hardness are given in Table 7. Considering the results, all main, quadratic and interaction parameters are significant. Figure 4(c) shows the normal probability plot for the hardness that does not indicate any unusual problem with normality assumptions. From DOE analysis, the regression Equation 4 was extracted for the hardness.

$$BHN = 39.297 - 1.378CIP + 5.346P + 1.228CIP \times P - 1.137CIP^2 - 0.213P^2 \quad (4)$$

**Table 7.** Analysis of variance for hardness

| Source of variation | Sum of squares | Degrees of freedom | Mean squares | *T* value | *F* value | *P* value |
|---|---|---|---|---|---|---|
| Regression | 401.658 | 5 | 80.332 | - | 1937.88 | 0.000 |
| CIP | 22.770 | 1 | 22.770 | -23.437 | 549.30 | 0.000 |
| P | 342.935 | 1 | 342.935 | 90.955 | 8272.82 | 0.000 |
| CIP×CIP | 29.627 | 1 | 29.627 | -26.734 | 714.70 | 0.000 |
| P×P | 1.043 | 1 | 1.043 | -5.016 | 25.16 | 0.002 |
| CIP×P | 6.027 | 1 | 6.027 | 12.058 | 145.39 | 0.000 |
| Residual | 0.290 | 7 | 0.041 | - | - | - |
| Lack-of-Fit | 0.187 | 3 | 0.062 | - | 2.41 | 0.208 |
| Pure Error | 0.103 | 4 | 0.026 | - | - | - |
| Total | 401.948 | 12 | - | - | - | - |
| $R^2$ = 99.93% | $R^2$ (adj) = 99.88% | | | | | |

According to Figure 9, by increasing the compaction pressure, regardless of the percentages of cast iron powder, the hardness increases. However, the situation is different in the case of varying the cast iron powder percentage. According to the surface plot, the hardness decreases with the increase of the cast iron powder percentage at low compaction pressures, while at high compaction pressures the hardness increases slowly with the increase of the cast iron powder percentage and the maximum hardness is achieved for the compact including 55% cast iron powder pressed at 800 MPa. The results show that the higher hardness of the cast iron powder with respect to the iron powder improves the hardness only at high compaction pressures, while

the low density of the mixtures including high amounts of the cast iron powder decreases the hardness at low compaction pressures.

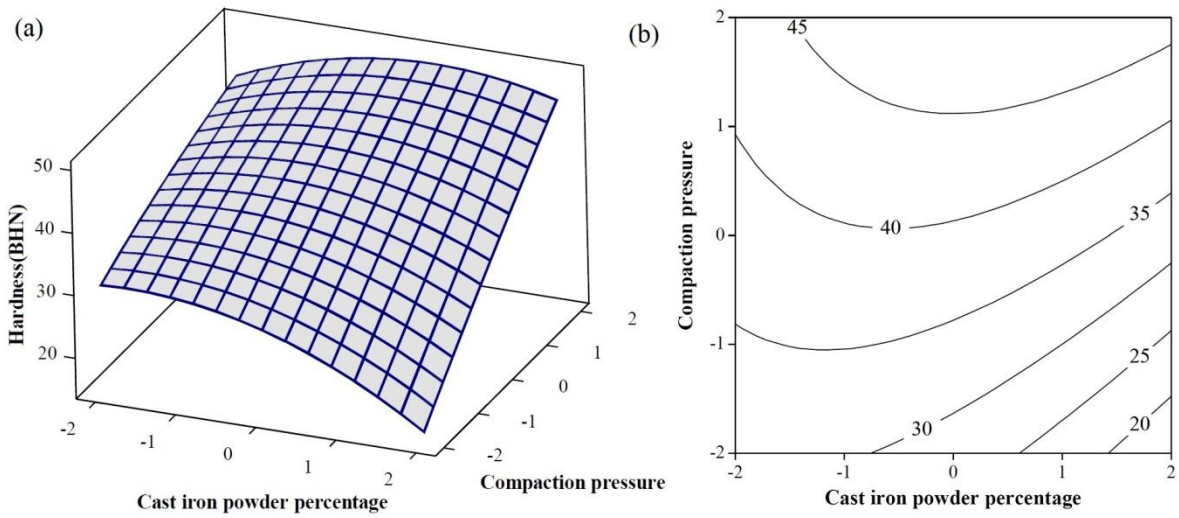


**Figure 9.** (a) Surface plot, and (b) contour plot, for hardness.

## 4. Optimization and validation

Maximum values of green density, green strength and hardness are obtained by optimizing the developed models. In addition, simultaneous optimization of different combinations of the responses is carried out in order to achieve simultaneous maximum values for green density, green strength and hardness. The validity of the optimized responses is evaluated by conducting two confirmation tests under optimum settings. Table 8 reports the maximized values of the responses, the optimum settings and the results of the confirmation tests. The bolded numbers in Table 8 are the optimized values and the other numbers in the columns named "opt." in each row are calculated from regression Equations of (2) to (4). All the italic numbers are the observed experimental results. The comparison of the predicted optimum results and the observed

confirmation results demonstrate that the developed models are very reliable as the all calculated errors are less than 4%.

**Table 8.** The optimized responses with the observed confirmation results

| Optimized response(s) | Factors | | Density(gr/cm$^3$) | | Strength(MPa) | | Hardness(BHN) | |
|---|---|---|---|---|---|---|---|---|
| | CIP(%) | P(MPa) | Opt. | Obs. | Opt. | Obs. | Opt. | Obs. |
| D | 30 | 800 | **6.42** | *6.58* | 13.78 | *14.25* | 42.43 | *41.27* |
| S | 30 | 800 | 6.42 | *6.58* | **13.78** | *14.25* | 42.43 | *41.27* |
| H | 54.65 | 800 | 6.24 | *6.41* | 12.01 | *12.36* | **49.39** | *50.19* |
| D,S | 30 | 800 | **6.42** | *6.58* | **13.78** | *14.25* | 42.43 | *41.27* |
| D,H | 52.63 | 800 | **6.28** | *6.15* | 12.15 | *12.55* | **49.34** | *48.11* |
| S,H | 43.33 | 800 | 6.36 | *6.54* | **12.81** | *12.49* | **47.91** | *48.75* |
| D,S,H | 41.31 | 800 | **6.35** | *6.52* | **12.95** | *13.38* | **47.34** | *46.65* |

## 5. Conclusions

The following conclusions are drawn based on this study:

1. Jet milled grey cast iron powders have the capability to be used in as-milled state in combination with iron powder for producing green compacts in industrial scales with acceptable green properties.
2. The proposed Equations (2) to (4) are accurate for predicting green density, green strength and hardness of the green compacts, respectively, within the selected range of the input parameters.
3. The green density and the green strength decrease with the increase of grey cast iron powder proportion. However, the hardness has a maximum value for the compact including 55% grey cast iron powder.
4. In the simultaneous optimization of the green density, green strength and hardness, the optimum set of the input parameters was obtained as 41% jet milled grey cast iron and 800 MPa of compaction pressure. The corresponding values 6.35 gr/cm$^3$, 12.95 MPa and 47 BHN were obtained, respectively. The errors between predicted values and the results of the confirmation tests were less than 4%.

## References


[1] Salak A, Riecansky V. Ferrous Powder Metallurgy. 1st ed. England: CISP, 1995.

[2] Hausner HH, Mal MK. Handbook of Powder Metallurgy. 2nd ed. New York: Chemical Pub. Co. Inc., 1982.

[3] Kjeldsteen P. Recycling of cast iron swarf by the powder metallurgy technique. Materials in Engineering 1982; 3: 335-340.

[4] Mamedov AT, Guliev AA. Production of powder from cast-iron chips and the features of preparation of parts from them, I: Production of powder, their structure, and properties. Powder Metallurgy and Metal Ceramics 1989; 7: 508-512.

[5] Karandikar DA. Processing of cast iron scrap from the diesel engine manufacturing industry by powder metallurgy techniques. Resources Conservation and Recycling 1991; 5: 61-71.

[6] Takeuchi E, Matsunaga M, Nakagawa T, Shuh Dai F. Friction and wear of sintered cast iron products. Wear 1982; 75: 303-312.

[7] Ghambari M, Emadi Shaibani M, Eshraghi N. Production of grey cast iron powder via target jet milling. Powder Technology 2012; 221: 318-324.

[8] Emadi Shaibani M, Ghambari M. Characterization and comparison of grey cast iron powder produced by target jet milling and high energy ball milling of machining scraps. Powder Technology 2011; 212: 278-283.

[9] Zozulya VD. Yaroshchuk TD, Zubarev VE, Bogdan LP, Bilobran BV. An investigation of the possibility of development of an antifriction iron-graphite material with the use of cast iron waste powders. Powder Metallurgy and Metal Ceramics 1990; 29:162-164.

[10] Mamedov AT, Aliev NA, Bakhyshev TA. Structure and properties of composite sintered material of the type iron-cast iron. Powder Metallurgy and Metal Ceramics 1993; 32 No. 1: 59-62.

[11] Bose A, mukunda PG. Bearings from machined cast iron swarf powder. Powder Metallurgy International1986; 18 No. 5: 333-337.

[12] Parucker ML, Costa CE. Study of the recycling grey cast iron swarf by powder metallurgy: an alternative for the development of new materials. Materials Science Forum 2006; 530-1: 3-9.

[13] Palanikumar K. Modeling and analysis for surface roughness in machining glassfibre reinforced plastics using response surface methodology. Materials and Design 2007; 28: 2611-2618.

[14] Yanhui Y, Dong L, Ziyan H, Zijian L. Optimization of Preform Shapes by RSM and FEM to Improve Deformation Homogeneity in Aerospace Forgings. Chinese Journal of Aeronautics 2010; 23: 260-267.

[15] Moradi M, Ghoreishi M, Frostevarg J, Kaplan AFH. An investigation on stability of laser hybrid arc welding. Optics and Lasers in Engineering 2013; 51: 481-487.

[16] Kumar S, Kumar P, Shan HS. Effect of evaporative pattern casting process parameters on the surface roughness of Al–7% Si alloy castings. Materials Processing Technology 2007; 182: 615-23.

[17] Li X, Zhao G, Guan Y, Ma M. Optimal design of heating channels for rapid heating cycle injection mold based on response surface and genetic algorithm. Materials and Design 2009; 30: 4317-4323.

[18] Senthilvelan T, Raghukandan K, Venkatraman A. Modelling of process parameters on the working of P/M copper performs. Materials Processing Technology 2003; 142: 767-772.

[19] Raghukandan K, Senthilvelan T. Analysis of P/M hollow extrusion using design of experiments. Materials Processing Technology 2004; 153–154: 416-419.

[20] Kumara S, Balasubramanian V. Developing a mathematical model to evaluate wear rate of AA7075/SiCp powder metallurgy composites. Wear 2008; 264: 1026-1034.

[21] Chatterjee D, Oraon B, Sutradhar G, Bose PK. Prediction of hardness for sintered HSS components using response surface method. Materials Processing Technology 2007; 190: 123-129.

[22] Klar E, Samal PK. Powder Metallurgy Stainless Steels: Processing, Microstructures, and Properties. 1st ed. ASM International, 2007.

[23] Montgomery DC. Design and Analysis of Experiments. 3rd ed. New York: John Wiley & Sons, 1991.

[24] Berns H, Theisen W. Ferrous Materials: Steels and Cast Iron. 1st ed. Germany: Springer, 2008.

[25] Upadhyaya GS. Powder metallurgy technology. 1st ed. England: CISP, 2002.

[26] ASM Handbook Volume 7. Powder Metal Technologies and Applications. ASM International, 1998.

[27] Khuri AI, Cornell JA. Response Surfaces Design and Analysis. 2nd ed. New York: Marcel Dekker, 1996.

[28] German RM. Powder metallurgy science. MPIF, 1994.

[29] Rosato AD, Vreeland T, Prinz FB. Manufacture of powder compacts. Inter. Materials Reviews 1991; 36 No. 2: 45–61.

[30] Kolaska H, Schulz P, beiss P, Ernst E. Investigations of die compaction. Powder Metallurgy International 1992; 24 No. 6: 30–35.